

# Magnetic-field control of the electric polarization in BiMnO<sub>3</sub>

I. V. Solovyev<sup>1,\*</sup> and Z. V. Pchelkina<sup>2</sup>

<sup>1</sup>National Institute for Materials Science, 1-2-1 Sengen, Tsukuba, Ibaraki 305-0047, Japan

<sup>2</sup>Institute of Metal Physics, Russian Academy of Sciences - Ural Division, 620041 Ekaterinburg GSP-170, Russia

(Dated: February 23, 2024)

We present the microscopic theory of improper multiferroicity in BiMnO<sub>3</sub>, which can be summarized as follows: (1) the ferroelectric polarization is driven by the hidden antiferromagnetic order in the otherwise centrosymmetric  $C2/c$  structure; (2) the relativistic spin-orbit interaction is responsible for the canted spin ferromagnetism. Our analysis is supported by numerical calculations of electronic polarization using Berry's phase formalism, which was applied to the low-energy model of BiMnO<sub>3</sub> derived from the first-principles calculations. We explicitly show how the electric polarization can be controlled by the magnetic field and argue that BiMnO<sub>3</sub> is a rare and potentially interesting material where ferroelectricity can indeed coexist and interplay with the ferromagnetism.

*Introduction.* Today, the term ‘multiferroics’ is typically understood in a broad sense, as the systems exhibiting spontaneous electric polarization and any type of magnetic ordering.<sup>1</sup> Such materials have a great potential for practical applications in magnetic memories, logic, and magnetoelectric sensors, and therefore attracted enormous attention recently. Beside practical motivations, there is a strong fundamental interest in unveiling the microscopic mechanism of coupling between electric polarization and magnetic degrees of freedom. Nevertheless, the combination of ferroelectricity and ferromagnetism, what the term ‘multiferroicity’ was originally introduced for, is rare. Such a combination would, for example, provide an easy way for manipulating the electric polarization  $\mathbf{P}$  by the external magnetic field, which is directly coupled to the net ferromagnetic (FM) moment, etc. The canonical example, where spontaneous electric polarization was believed to coexist with the FM ground state, is BiMnO<sub>3</sub>. However, the origin of such coexistence is largely unknown. Originally, the ferroelectric (FE) behavior in BiMnO<sub>3</sub> was attributed to the highly distorted perovskite structure stabilized by the Bi6s “lone pairs”.<sup>2</sup> However, more recent experimental studies (Ref. 3) and first-principles calculations (Ref. 4) suggested that the atomic displacements alone result in the centrosymmetric  $C2/c$  structure, which is incompatible with the ferroelectricity. In our previous papers (Refs. 5 and 6) we put forward the idea that the ferroelectricity in BiMnO<sub>3</sub> could be improper and associated with some hidden antiferromagnetic (AFM) order. The purpose of this work is to provide the complete quantitative explanation for the appearance and behavior of the FE polarization in BiMnO<sub>3</sub>.

*Method.* The basic idea of our approach is to construct an effective Hubbard-type model

$$\hat{\mathcal{H}} = \sum_{ij} \sum_{\alpha\beta} t_{ij}^{\alpha\beta} \hat{c}_{i\alpha}^\dagger \hat{c}_{j\beta} + \frac{1}{2} \sum_i \sum_{\alpha\beta\gamma\delta} U_{\alpha\beta\gamma\delta} \hat{c}_{i\alpha}^\dagger \hat{c}_{i\gamma}^\dagger \hat{c}_{i\beta} \hat{c}_{i\delta} \quad (1)$$

for the Mn3d-bands near the Fermi level and to include the effect of all other (“inactive”) states to the definition of the model parameters of the Hamiltonian  $\hat{\mathcal{H}}$ . Thus, the model is constructed in the basis of 40 Wan-

nier functions in each unit cell (including three  $t_{2g}$ - and two  $e_g$ -orbitals for each spin and for each of the four Mn-sites), by starting from the electronic structure in the local-density approximation (LDA). The Greek symbols denote the combination of spin and orbital indices. All parameters of  $\hat{\mathcal{H}}$  are defined rigorously, on the basis of the density functional theory (DFT). The details can be found in the review article (Ref. 7) and in our previous papers (Refs. 5 and 6). Briefly, the one-electron part ( $t_{ij}^{\alpha\beta}$ ) is derived by using the generalized downfolding method. One of important parameters in  $t_{ij}^{\alpha\beta}$  is the large (about 1.5 eV) crystal-field splitting between two  $e_g$ -levels, which is caused by the Jahn-Teller distortion and manifests itself in the orbital ordering. The screened Coulomb interactions ( $U_{\alpha\beta\gamma\delta}$ ) are obtained by combining the constrained DFT technique with the random-phase approximation (RPA):<sup>7</sup> namely, the screening by outer electrons (such as 4sp-electrons of transition metals) and the change of spacial extension of the atomic wavefunctions upon the change of occupation numbers can be easily taken into account by solving Kohn-Sham equations within constrained DFT approach. On the other hand, the “self-screening” by the same type of electrons, which contribute to other bands due to the hybridization effects (for example, the 3d-electrons in the oxygen band will strongly screen the Coulomb interactions in the 3d-band near the Fermi level), is included in the perturbative RPA treatment. The self-screening is very important in solids and substantially reduces the value of the effective Coulomb repulsion  $U$  (defined as the screened Slater integral  $F^0$ ) in the 3d-band of manganites.<sup>8</sup> In BiMnO<sub>3</sub>, it is only about 2.3 eV,<sup>5</sup> that has important consequences on the behavior of interatomic magnetic interactions.

The model (1) is solved in the Hartree-Fock (HF) approximation:<sup>7</sup>

$$(\hat{t}_{\mathbf{k}} + \hat{\mathcal{V}}) |C_{n\mathbf{k}}\rangle = \varepsilon_{n\mathbf{k}} |C_{n\mathbf{k}}\rangle,$$

where  $\hat{t}_{\mathbf{k}}$  is the Fourier image of  $\hat{t}_{ij} = \|t_{ij}^{\alpha\beta}\|$  and, if necessary, includes the relativistic spin-orbit coupling (SOC),  $\hat{\mathcal{V}}$  is the self-consistent HF potential, and  $|C_{n\mathbf{k}}\rangle$  is the eigenvector in the basis of Wannier functions (where the

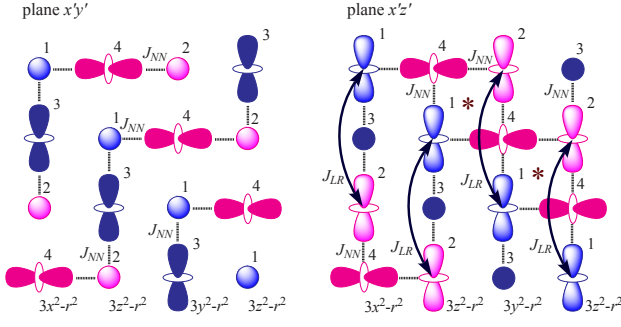


FIG. 1. (Color online) Schematic view on the orbital ordering and corresponding interatomic magnetic interactions in the pseudocubic  $x'y'$  and  $z'x'$  planes. In the unit cell of  $\text{BiMnO}_3$ , there are four Mn sites (indicated by numbers), which form two inequivalent groups: (1,2) and (3,4). The nearest-neighbor FM interactions  $J_{NN}$  operate in the hatched bonds. The atoms involved in the long-range AFM interactions  $J_{LR}$  are denoted by arrows. The inversion centers are marked by '\*'.

spin indices are included in the definition of  $n$ ).<sup>9</sup>

Once the orbital degeneracy is lifted by the strong lattice distortion, the HF theory provides a good approximation for the ground-state properties. The effect of correlation interactions, which can be treated as a perturbation to the HF solution,<sup>7</sup> on the magnetic ground state of manganites is partially compensated by the magnetic polarization of the oxygen states: if the former tend to stabilize AFM structures, the latter favors the FM alignment.<sup>8</sup> Due to this compensation, the mean-field HF theory, formulated for the minimal  $3d$ -model, appears to be rather successful for the ground state of manganites.

*Magnetism and the inversion symmetry breaking.* First, let us explain the main idea of our work.<sup>5,6</sup> What is the possible origin of multiferroic behavior of  $\text{BiMnO}_3$  and how can it be controlled by the magnetic field?

(1) The lattice distortion leads the orbital ordering, which is schematically shown in Fig. 1 in two pseudocubic planes (the orbital ordering in the  $y'z'$ -plane is similar to the one in the  $z'x'$ -plane). This orbital ordering pre-determines the behavior of interatomic magnetic interactions, which obey some general principles, applicable for manganites with both monoclinic ( $C2/c$ ) and orthorhombic ( $Pnma$ ) structure,<sup>5,8</sup> namely: besides conventional nearest-neighbor interactions (shown by hatched lines), one can expect some longer-range (LR) interactions between remote Mn-atoms, which operate via intermediate Mn-sites. These sites are shown by arrows.

(2) Why should the LR-interactions exist? The answer is directly related to the fact that the on-site Coulomb repulsion  $U$  is not particularly large. Therefore, besides conventional superexchange (SE), there are other interactions, which formally appear in the higher orders of the  $1/U$ -expansion and connect more remote sites. This mechanism is rather similar to the SE interaction via intermediate oxygen sites, but the role of the oxygen states

is played by the unoccupied  $e_g$ -orbitals of the intermediate Mn-sites.<sup>8</sup> By mapping HF total energies onto the Heisenberg model, one can obtain the following parameters of interatomic magnetic interactions:<sup>5,10</sup>  $J_{NN} \sim 5$  and 6 meV (where slightly different values correspond to different bonds) and  $J_{LR} \sim -3$  meV. Thus, these interactions are at least comparable. Besides them, there are finite (of the order  $-1$  meV) interactions in the bonds 1-2 and 4-4 across the inversion center, which finally define the type of the magnetic ground state of  $\text{BiMnO}_3$ .

(3) Without SOC, the LR interactions tend to stabilize the AFM  $\uparrow\downarrow\uparrow$  structure (where the arrows denote the directions of spins for the four Mn-sites in the unit cell). This AFM order destroys the inversion centers (shown by '\*' in Fig. 1) and thus should give rise to the FE polarization. Since the  $\uparrow\downarrow\uparrow$  structure satisfies the symmetry operation  $\hat{T} \otimes \{m_y | \mathbf{R}_3/2\}$  (where  $m_y$  is the mirror reflection  $y \rightarrow -y$  associated with the one half of the monoclinic translation  $\mathbf{R}_3$ , and  $\hat{T}$  in the nonrelativistic case flips the directions of spins, which are not affected by  $m_y$ ),  $\mathbf{P}$  is expected to lie in the  $zx$ -plane.<sup>11</sup>

(4) Thus, the FE behavior in  $\text{BiMnO}_3$  should be caused by the AFM order. However, this conclusion seems to contradict to the FM ground state of  $\text{BiMnO}_3$ .<sup>3</sup> The contradiction can be reconciled by considering the relativistic SOC, which is responsible for the weak ferromagnetism. Since the FM component is additionally stabilized by the isotropic interactions  $J_{NN}$ , the ferromagnetism is not so "weak", and the resulting magnetic structure, obtained in the HF calculations for the low-energy model, is strongly noncollinear (Fig. 2). It belongs to the space group  $Cc$ , where the only nontrivial symmetry operation is  $\{m_y | \mathbf{R}_3/2\}$  and the magnetic moments in the relativistic case are transformed by  $m_y$  as auxiliary vectors. Thus, the net FM moment is aligned along the  $y$ -axis, while the  $x$ - and  $z$ -components form the AFM structure. Other magnetic configurations have higher energies. The details can be found in Ref. 6.

By summarizing this part, the  $C2/c$  symmetry of  $\text{BiMnO}_3$  is spontaneously broken by the hidden AFM order. The true magnetic ground-state of  $\text{BiMnO}_3$  is strongly noncollinear, where the FM order along the  $y$ -axis coexists with the AFM order, and related to it FE polarization, along the  $x$ - and  $z$ -axes. Our scenario not only explains the coexistence of ferroelectricity and ferromagnetism, but also shows how the electric polarization  $\mathbf{P}$  (and the symmetry of  $\text{BiMnO}_3$ ) can be controlled by the external magnetic field  $\mathbf{B}=(0, B_y, 0)$  coupled to the FM moment. This basic idea was formulated in Ref. 6. In the present work we are able to provide the numerical estimates for  $\mathbf{P}$  and to discuss its behavior in details.

*Electric polarization.* Since the crystal structure of  $\text{BiMnO}_3$  has the inversion symmetry, there will be no ionic contribution to  $\mathbf{P}$ , and the main mechanism, which will be considered below, is of purely electronic origin. In principle, the magneto-elastic interactions in the  $\uparrow\downarrow\uparrow$  structure may cause the atomic displacements away from the centrosymmetric positions and give rise to the ionic

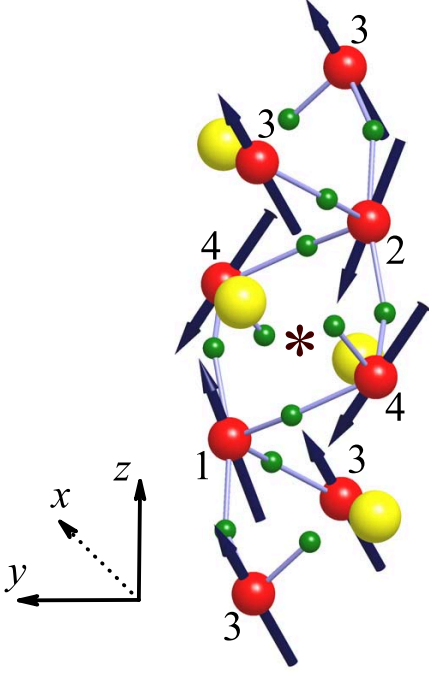


FIG. 2. (Color online) Fragment of crystal and magnetic structure corresponding to the lowest HF energy. The Bi-atoms are indicated by the big light grey (yellow) spheres, the Mn-atoms are indicated by the medium grey (red) spheres, and the oxygen atoms are indicated by the small grey (green) spheres. The directions of spin magnetic moments are shown by arrows. The inversion center is marked by the symbol '\*'. The left lower part of the figure explains the orientation of the Cartesian coordinate frame.

term. Nevertheless, such calculations would require the full structure optimization, which cannot be easily incorporated in the model analysis. The first-principles calculations for  $\text{HoMnO}_3$  show that electronic and ionic terms are at least comparable.<sup>12</sup> Thus, we expect that the electronic contribution alone could provide a good semi-quantitative estimate for  $\mathbf{P}$ . Moreover, the behavior of electronic contribution presents a fundamental interest as it allows one to explain how  $\mathbf{P}$  in improper multiferroics is induced solely by the magnetic symmetry breaking.

The modern theory of electric polarization allows one to relate the change of  $\mathbf{P}$  to the Berry phase of Bloch eigenstates.<sup>13–15</sup> It is particularly convenient to use the formulation by Resta, where the Berry phase is computed on the discrete grid of  $\mathbf{k}$ -points, generated by the  $N_1 \times N_2 \times N_3$  divisions of the reciprocal lattice vectors  $\{\mathbf{G}_a\}$ .<sup>15</sup> Then, the position of each point in the Brillouin zone is specified by three integer indices ( $0 \leq s_a < N_a$ ):

$$\mathbf{k}_{s_1, s_2, s_3} = \frac{s_1}{N_1} \mathbf{G}_1 + \frac{s_2}{N_2} \mathbf{G}_2 + \frac{s_3}{N_3} \mathbf{G}_3,$$

and components of the electric polarization in the curvilinear coordinate frame formed by  $\mathbf{G}_1$ ,  $\mathbf{G}_2$  and  $\mathbf{G}_3$  can

be obtained as<sup>15</sup>

$$\Delta P_a = -\frac{1}{V} \frac{N_a}{N_1 N_2 N_3} [\gamma_a(\infty) - \gamma_a(0)], \quad (2)$$

where  $V$  is the unit cell volume,

$$\gamma_1 = - \sum_{s_2=0}^{N_2-1} \sum_{s_3=0}^{N_3-1} \text{Im} \ln \prod_{s_1=0}^{N_1-1} \det S(\mathbf{k}_{s_1, s_2, s_3}, \mathbf{k}_{s_1+1, s_2, s_3}),$$

and similar expressions hold for  $\gamma_2$  and  $\gamma_3$ . Eq. (2) implies that the only meaningful quantity in the bulk is the polarization difference between two states that can be connected by an adiabatic switching process.<sup>13–15</sup>

In the present case,  $S = \|\langle C_{n\mathbf{k}} | C_{n'\mathbf{k}'} \rangle\|$  is the overlap matrix, constructed from the HF eigenvectors  $|C_{n\mathbf{k}}\rangle$  in the occupied part of spectra, taken in two neighboring  $\mathbf{k}$ -points:  $\mathbf{k} = \mathbf{k}_{s_1, s_2, s_3}$  and  $\mathbf{k}' = \mathbf{k}_{s_1+1, s_2, s_3}$  for  $\gamma_1$ , etc.<sup>16</sup> The polarization (2) was first computed in the curvilinear coordinate frame and then transformed to the cartesian frame shown in Fig. 2.<sup>11</sup> In all the calculations, we used the mesh of  $72 \times 72 \times 36$  points in the Brillouin zone.

Without SOC, the AFM alignment of spins at the sites 1 and 2 yields finite polarization. However, the symmetry of the system also depends on the magnetic configuration in the sublattice 3-4. As discussed above, the electric polarization in the  $\uparrow\downarrow\uparrow$  structure lies in the  $zx$ -plane ( $P_x = 2.1 \mu\text{C}/\text{cm}^2$  and  $P_z = 0.1 \mu\text{C}/\text{cm}^2$ ). The  $\uparrow\downarrow\uparrow$  structure can be transformed to the  $\uparrow\downarrow\downarrow$  one with the same energy by the symmetry operation  $\{C_y^2 | \mathbf{R}_3/2\}$  (where  $C_y^2$  is the  $180^\circ$  rotation around the  $y$ -axis), which changes the direction of  $\mathbf{P}$ :  $P_{x(z)} \rightarrow -P_{x(z)}$ . On the other hand, the  $\uparrow\downarrow\downarrow$  structure (which has higher energy) is transformed to itself by  $\{C_y^2 | \mathbf{R}_3/2\}$ , and corresponding electric polarization will be parallel to the  $y$ -axis ( $P_y = 4.8 \mu\text{C}/\text{cm}^2$ ). Other magnetic structures, characterized by the FM alignment of spins at the sites 1 and 2 (such as  $\uparrow\uparrow\uparrow$  and  $\uparrow\uparrow\downarrow$ ), preserve the inversion symmetry and result in zero net polarization.

Without SOC, one can easily evaluate separate contributions to  $\mathbf{P}$  of the states with the spin  $\uparrow$  and  $\downarrow$ . For the  $\uparrow\downarrow\uparrow$  structure, the vector of the electric polarization takes the following form:  $\mathbf{P}^{\uparrow, \downarrow} = \frac{1}{2}(P_x, \pm P_y, P_z)$ , where  $P_y = 5.7 \mu\text{C}/\text{cm}^2$ , and the values of  $P_x$  and  $P_y$  are listed above. This result is very natural, because the distribution of the electron density for each spin does not have any symmetry and, therefore, the electric polarization  $\mathbf{P}^{\uparrow, \downarrow}$  has all three components. On the other hand, the electron density with the spin  $\uparrow$  in the  $\uparrow\downarrow\uparrow$  AFM state can be transformed to the one with the spin  $\downarrow$  by the symmetry operation  $\{m_y | \mathbf{R}_3/2\}$  and, therefore,  $P_y^\uparrow = -P_y^\downarrow$ . Thus, in the total polarization  $\mathbf{P} = \mathbf{P}^\uparrow + \mathbf{P}^\downarrow$ , the  $x$ - and  $z$ -components with different spins will sum up, while the largest  $y$ -components will cancel each other.

Furthermore, one can evaluate the individual contributions to  $\mathbf{P}$  coming from the  $t_{2g}$ -band, which is separated by an energy gap from the  $e_g$ -band.<sup>5</sup> This yields:  $P_x^{t_{2g}} = -0.8 \mu\text{C}/\text{cm}^2$  and  $P_z^{t_{2g}} = -0.3 \mu\text{C}/\text{cm}^2$ . Thus,

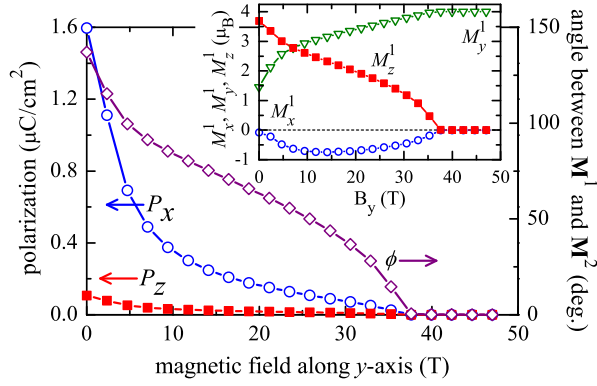


FIG. 3. (Color online) Magnetic-field dependence of the electric polarization, the angle  $\phi$  between spin magnetic moments at the Mn-sites 1 and 2, and the vector of magnetic moment at the site 1 (shown in the inset).

the  $t_{2g}$ -band is polarized *opposite* to the  $e_g$ -band, that substantially reduces the value of  $\mathbf{P}$ .

The SOC results in the canting of spins away from the collinear  $\uparrow\downarrow\uparrow$  state and towards the FM configuration. It will *reduce* the value of  $\mathbf{P}$ . In the HF ground-state (see Fig. 2), the angle  $\phi$  between spin magnetic moments at the sites 1 and 2 is  $137^\circ$ , and the electric polarization is reduced till  $P_x = 1.6 \mu\text{C}/\text{cm}^2$  and  $P_z = 0.1 \mu\text{C}/\text{cm}^2$ . This effect can be further controlled by the magnetic field, which is applied along the  $y$ -axis and saturates the FM magnetization. Since the absolute value of the local magnetic moment is nearly conserved, the increase of the FM component along the  $y$ -axis will be compensated by the decrease of two AFM components along the  $x$ - and

$z$ -axes. The corresponding FE polarization will also decrease. Results of HF calculations in the magnetic field are shown in Fig. 3.<sup>17</sup> Sufficiently large magnetic field ( $\sim 35$  Tesla) will align the magnetic moments at the sites 1 and 2 ferromagnetically ( $\phi=0$ ) and restore the  $C2/c$  symmetry.<sup>6</sup> The electric polarization follows the change of  $\phi$  and complete disappears when  $\phi=0$ . However, the decline of  $\mathbf{P}$  is much steeper: for example,  $P_x$  and  $P_z$  are reduced by factor two already in the moderate field  $B_y \sim 5$  Tesla, corresponding to  $\phi \sim 100^\circ$ . Moreover,  $P_z$  is always substantially smaller than  $P_x$ .

*Concluding remarks.* We have proposed the microscopic theory of improper multiferroicity in  $\text{BiMnO}_3$ , which is based on the inversion symmetry breaking by the hidden AFM order. We have estimated the FE polarization and explicitly shown how it can be controlled by the magnetic field. Our scenario still needs to be checked experimentally, and apparently one important question here is how to separate the intrinsic ferroelectricity in  $\text{BiMnO}_3$  from extrinsic effects, caused by the defects. For example, the values of the FE polarization obtained in the present work, although comparable with those calculated for other improper ferroelectrics on the basis of manganites,<sup>12</sup> are substantially larger than the experimental value  $0.062 \mu\text{C}/\text{cm}^2$  (at 87 K), which was reported so far for  $\text{BiMnO}_3$ .<sup>18</sup> Nevertheless, we believe that systematic study of manganites with the monoclinic  $C2/c$  symmetry and finding conditions, which would lead to the practical realization of scenario proposed in our work, presents a very important direction, because it gives a possibility for combining and intermanipulating the *ferroelectricity* and *ferromagnetism* in one sample.

*Acknowledgements.* This work is partly supported by Grant-in-Aid for Scientific Research (C) No. 20540337 from MEXT, Japan and Russian Federal Agency for Science and Innovations, grant No. 02.740.11.0217.

\* SOLOVYEV.Igor@nims.go.jp

<sup>1</sup> D. Khomskii, *Physics* **2**, 20 (2009).

<sup>2</sup> R. Seshadri and N. A. Hill, *Chem. Mater.* **13**, 2892 (2001).

<sup>3</sup> A. A. Belik *et al.*, *J. Am. Chem. Soc.* **129**, 971 (2007).

<sup>4</sup> P. Baettig, R. Seshadri and N. A. Spaldin, *J. Am. Chem. Soc.* **129**, 9854 (2007).

<sup>5</sup> I. V. Solov'yev and Z. V. Pchelkina, *New J. Phys.* **10**, 073021 (2008).

<sup>6</sup> I. V. Solov'yev, Z. V. Pchelkina, *Pis'ma Zh. Eksp. Teor. Fiz.* **89**, 701 (2009) [*JETP Lett.* **89**, 597 (2009)].

<sup>7</sup> I. V. Solov'yev, *J. Phys.: Condens. Matter* **20**, 293201 (2008).

<sup>8</sup> I. Solov'yev, *J. Phys. Soc. Jpn.* **78**, 054710 (2009).

<sup>9</sup> The Fourier image of  $\hat{t}_{ij}$  was defined as  $\hat{t}_{\mathbf{k}} = \sum_j \hat{t}_{ij} \exp(-i\mathbf{k} \cdot \mathbf{R}_{ij})$ , where  $\mathbf{R}_{ij}$  is the radius-vector between sites  $i$  and  $j$ . Such a definition guarantees that the eigenvectors  $|C_{n\mathbf{k}}\rangle$  are periodic in both direct and reciprocal space, as it is required for calculations of  $\mathbf{P}$ .<sup>13-15</sup>

<sup>10</sup> The spin model is defined as  $\mathcal{H}_S = -\sum_{\langle ij \rangle} J_{ij} \mathbf{e}_i \cdot \mathbf{e}_j$ , where  $\mathbf{e}_i$  and  $\mathbf{e}_j$  are the *directions* spins.

<sup>11</sup> We use the following setting for the monoclinic translations:  $\mathbf{R}_{1,2} = \frac{1}{2}(\sin \beta a, \mp b, \cos \beta a)$  and  $\mathbf{R}_3 = (0, 0, c)$ . The positions of four Mn atoms in the unit cell are specified by the vectors:  $\boldsymbol{\tau}_1 = y_{\text{Mn}}(\mathbf{R}_1 - \mathbf{R}_2) + \frac{1}{4}\mathbf{R}_3$ ,  $\boldsymbol{\tau}_2 = -\boldsymbol{\tau}_1$ ,  $\boldsymbol{\tau}_3 = \frac{1}{2}\mathbf{R}_1$ , and  $\boldsymbol{\tau}_4 = \frac{1}{2}(\mathbf{R}_2 + \mathbf{R}_3)$ . The experimental structure parameters were taken from Ref. 3.

<sup>12</sup> S. Picozzi *et al.*, *Phys. Rev. Lett.* **99**, 227201 (2007).

<sup>13</sup> D. Vanderbilt and R. D. King-Smith, *Phys. Rev. B* **48**, 4442 (1993).

<sup>14</sup> R. Resta, *Rev. Mod. Phys.* **66**, 899 (1994).

<sup>15</sup> R. Resta, *J. Phys.: Condens. Matter* **22**, 123201 (2010).

<sup>16</sup> Strictly speaking, there will be two contributions to  $\mathbf{P}$ : one is caused by the evaluation of  $|C_{n\mathbf{k}}\rangle$  in the  $\mathbf{k}$ -space and the other one is the contribution of  $\{W^\alpha\}$  (the Wannier basis of the low-energy model), which is expressed in terms of the matrix elements  $\langle W^\alpha | \mathbf{r} | W^\beta \rangle$ . Since the low-energy model is constructed by starting from the nonmagnetic LDA band structure, which preserves the parity of  $\{W^\alpha\}$ , these matrix elements will vanish.

<sup>17</sup> The interaction term with the magnetic field is given by

$\hat{\mathcal{H}}_B = -\mu_B \mathbf{B} \cdot (2\hat{\mathbf{s}} + \hat{\mathbf{l}})$ , where  $\hat{\mathbf{s}}$  and  $\hat{\mathbf{l}}$  are the operators of spin and orbital angular momentum, respectively.

<sup>18</sup> A. Moreira dos Santos *et al.*, Solid State Commun. **122**, 49 (2002).